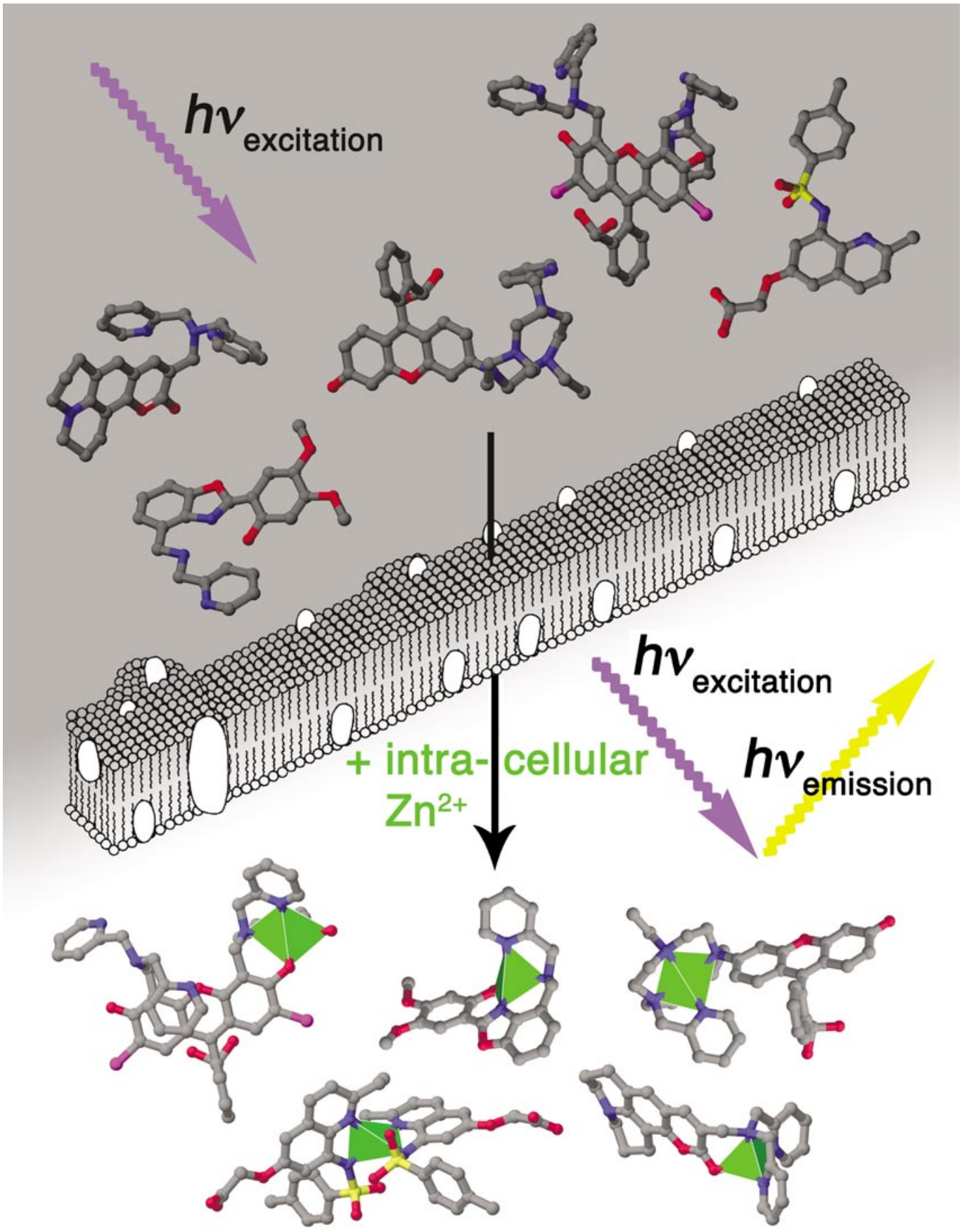

Illuminating Zinc in Biological Systems

DOI: 10.1002/chem.200400599

Illuminating Zinc in Biological Systems**

Nathaniel C. Lim,[a] Hedley C. Freake,[b] and Christian Brückner*[a]

Abstract: Zinc is the second most abundant transition metal in the human body, fulfilling a multitude of biological roles, but the mechanisms underlying its physiology are poorly understood. The lack of knowledge is, in part, due to the hitherto limited techniques available to track zinc in biological systems. The recent emergence of a number of zinc-specific molecular sensors has provided a new tool to image zinc in live cells and tissue samples. This contribution highlights the concepts behind using zinc-specific fluorescent molecular sensors to gain information about zinc action in biological samples, and provides representative examples of images recorded.

Keywords: chemosensors · fluorescent probes · imaging agents · sensors · zinc

Introduction

Physiology of zinc: Zinc is only moderately abundant in nature, ranking 23rd of the elements. Zinc is, however, following iron, the second most abundant transition metal in the body. In total, the adult human body contains 2–3 g zinc. The pronounced Lewis acid characteristics of the Zn^{2+} ion, its single redox state, and the flexibility of its coordination sphere with respect to geometry and number of ligands associated, combined with the kinetic lability of coordinated ligands, are responsible for its broad utility within proteins of the body. While other trace elements may share some of these properties, none share them all.

Probably thousands of proteins contain zinc.[1] All six International Union of Biochemistry class of enzymes are represented. The structures of well over 200 zinc-containing enzymes have now been characterized.[2] Zinc proteins can be divided into several groups according to the role played by zinc within the protein. In the catalytic group (e.g., carbonic anhydrase and carboxypeptidase A), zinc is a direct participant in the catalytic function of the enzyme. In enzymes with structural zinc sites (e.g., protein kinase C), one or more metal ions ensure appropriate folding for bioactivity. Enzymes in which zinc serves a co-catalytic function (e.g., superoxide dismutase), one or several zinc ions may be used for catalytic, regulatory, and structural functions. In addition, there are a large number of transcription factors that utilize zinc, the so-called zinc fingers.[3] Zinc is found associated with membrane lipids, DNA, and RNA, but the functions of these zinc pools are not clear.

Considering the wide variety of metabolic functions requiring zinc, it is not surprising that any zinc deficiency or imbalanced zinc distribution within the body, organ or cell, leads to a broad range of pathologies. Human zinc deficiency was first discovered almost 50 years ago by Prasad and co-workers.[4] They described a syndrome of stunted growth and sexual immaturity in adolescent boys. The extent to which zinc deficiency conditions persist today is difficult to estimate because of the lack of a suitable biochemical marker of zinc status. However, the World Health Organization estimates that more than 40% of young children in many parts of Africa and Asia have stunted growth and this can often be associated with limited dietary zinc.[5] Zinc has also been reported to increase growth rates in children in the United States.[6] In addition to growth, numerous other body functions are affected, including immune, endocrine, and gastro-enterological systems.[1] These effects often interact with other diseases ranging from diarrhea to AIDS, worsening the resultant pathologies.[7]

While the structural biochemistry of zinc within proteins and the pathology of zinc deficiency have both been reasonably well described, large gaps in understanding the connections between the two exist. In addition, the roles that zinc play in many physiological processes, ranging from insulin

[a] Dr. N. C. Lim, Prof. Dr. C. Brückner
Department of Chemistry
University of Connecticut, Storrs, CT 06269-3060 (USA)
Fax: (+1) 860-486-2981
E-mail: c.bruckner@uconn.edu

[b] Prof. Dr. H. C. Freake
Department of Nutritional Sciences
University of Connecticut, Storrs, CT 06269-4017 (USA)

[**] Because of the overview nature of this paper, references are not exhaustive and primarily serve as entry points to the relevant literature. Recent comprehensive listings of zinc sensors are available, see reference [14]. We apologize to all the groups who have contributed to the field and whose work was not explicitly mentioned.

 DOI: 10.1002/chem.200400599

secretion, apoptosis, neurodegenerative disorders, taste, and smell function are not well understood. Understanding of zinc homeostasis and the regulation of its passage into and out of cells is improving with the discovery zinc transporters,[8] but many questions remain about how zinc is supplied to its protein partners.[9] Much more needs to be learned about zinc speciation, compartmentalization, and the regulation and the mechanisms of the intracellular trafficking of zinc.[10]

While the total concentration of zinc in a cell is relatively high, the concentration of "free" zinc, that is, the fraction of Zn^{2+} not strongly bound to proteins, is extremely low and tightly controlled.[11,12] In fact, the measurement of the extraordinary affinity of the bacterial zinc sensor/regulatory protein ZntR has led to an apparent physiological paradox. The concentrations of free Zn^{2+} that activate the ZntR are about six orders of magnitude lower than one zinc ion per cell![11,13] ZntR turns on the expression of zinc efflux pumps. This then raises the question of how zinc-dependent proteins of lower affinity to zinc than ZntR receive their required zinc if extremely low zinc concentrations already engage the zinc efflux pumps. The paradox is solved when considering that a cell is not at thermodynamic equilibrium. Thus employing a kinetic model that involves ligand exchange reactions between a number of zinc-binding proteins, including zinc chaperones, can explain the control of the intracellular zinc quota.[11,13]

Total cellular zinc can be relatively easily determined by standard analytical techniques such as AAS or ICP-MS, but the determination of the "free" or "available" Zn^{2+} concentrations has proved difficult using classic techniques. This is because cell fractionation can readily lead to cross-contamination of the kinetically labile metal ion between intracellular sites. Thus, the knowledge gap between the structural chemistry of zinc and zinc homeostasis and action is, at least in part, due to the lack of techniques for tracking Zn^{2+} in biological systems. This has led to the emergence of zinc-specific molecular sensors, which can make zinc "visible" in tissue or even in live cells.[14]

Spectroscopically silent zinc: The d^{10} electron configuration of the Zn^{2+} ion, the only zinc ion found in biological systems, has a number of practical implications for its detection. Zn^{2+} is colorless as it is devoid of d–d transitions. The Zn^{2+} ion is very stable and undergoes redox reactions only under extreme conditions, excluding the occurrence of ligand-to-metal charge-transfer bands in its complexes. These effects render UV-visible spectroscopy unsuitable for the detection of "free" or complexed Zn^{2+}. Zinc is also diamagnetic in all its compounds, prohibiting, for instance, EPR spectroscopy or magnetometric measurements. The d^{10} ion is not subject to ligand field stabilization effects, making it extremely flexible with respect to the coordination geometries it can adopt in its complexes, and rendering it kinetically labile, allowing for rapid ligand exchange reactions. Finally, the major naturally occurring isotopes have zero nuclear spin, they are NMR silent.

Much of what is known about the structure and function of Zn^{2+}-containing proteins has been gleaned from X-ray crystal structures, X-ray absorption data (EXAFS), and isomorphous substitution experiments in which the Zn^{2+} was replaced by traceable metal ions.[12] None of these techniques are suitable for the tracking of Zn^{2+} in cells and organisms. The use of the zinc radioisotope ^{65}Zn has allowed cell studies on bulk zinc uptake and egress, but this does not permit the direct observation of the temporal and spatial distribution of zinc in live cells and questions of isotope equilibration with internal pools arise.[15] One technique to spectroscopically visualize zinc is the use of zinc-specific fluorescent molecular sensors.

Molecular sensors: A molecular sensor (also referred to as a chemosensor) is a molecule capable of transforming chemical information, such as presence or concentration of a specific sample component, into an analytically useful signal.[16,17] A metal-ion chemosensor comprises a metal-ion recognition site and a signal transduction domain that is triggered upon metal-ion binding. For instance, metal binding triggers intense fluorescence in the sensor, while the unbound sensor is nonfluorescent (Figure 1).

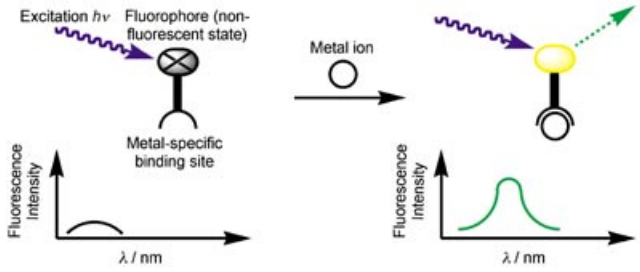

Figure 1. Schematic representation of CHEF-type fluorescent molecular metal sensor.

One realization of such a "switch-on" probe relies on a photoinduced electron-transfer (PET) mechanism. Such a mechanism involves the deactivation of the excited state of a fluorophore by addition of an electron to one of its excited-state frontier orbitals. This leaves the fluorophore in a reduced, nonemissive state. For example, the free electron pair of an amino group attached in a benzylic position to a fluorophore may quench its fluorescence intramolecularly as a result of a PET process. Metal coordination to the amino group renders it a less efficient electron donor. This makes PET-type fluorescence quenching less probable or interrupts it all together. Thus, the native fluorescence of the fluorophore is restored. This signaling event should be highly sensitive and selective for the analyte. Sensors operating according to this principle have become known as CHEF-type sensors (chelation-enhanced fluorescence).[16,17]

Chemosensors principally allow the tracking of zinc in live cells or organ preparations using fluorescence microscopy.[18] The enormous utility of metallochemosensors in biology has been previously demonstrated for Ca^{2+}, another spectroscopically silent metal ion.[19]

Fluorescent Sensing of Zinc in Biological Systems

Requirements for a zinc chemosensor suitable to probe biological samples

Desired optical properties: The ideal chemosensor for zinc is nonfluorescent in the free-base form and highly fluorescent when coordinated to zinc. The best established zinc chemosensors, the 8-aminoquinoline-based sensors **1**–**3**, show about a 300-fold increase in their fluorescence intensity upon *N*,*N*-chelation of zinc, an increase rarely matched by other sensors.[20–22] Further, these sensors are exquisitely sensitive for zinc, capable of detecting concentrations down to 4 pM.[21]

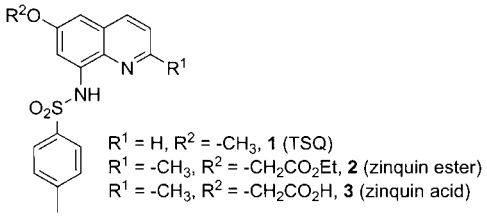

Figure 2 shows a typical, more moderate, increase of fluorescence upon titration with increasing amounts of Zn^{2+}, here illustrated using the fluorescein-based sensor Zinpyr-1

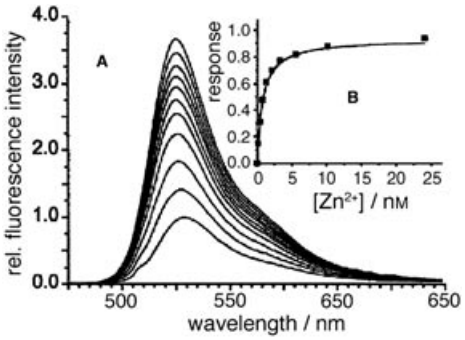

Figure 2. A: Fluorescence emission response of Zinpyr-1 (**4**) to buffered Zn^{2+} solutions. B: Fluorescence response obtained by integrating the emission spectra between 509 and 650 nm. $\lambda_{excitation}$ at 507 nm. For further experimental details, see Walkup et al.[23] (figure used with permission).

(**4**), introduced by Lippard and co-workers.[23] Upon binding of Zn^{2+}, no spectral shift is observed, merely a gradual switching on of the fluorescence with increasing zinc concentration until the limiting stoichiometry of the metal–ligand complex is reached. Despite the smaller increase in fluorescence intensity, Zinpyr (and other rhodamine- and fluorescein-based sensors)[24–26] have a major advantage over aminoquinoline-based systems, such as **1** and **2** and related sensors.[27,28] The excitation wavelength $\lambda_{excitation}$ for Zinpyr-1 is 507 nm, while the quinoline **2** requires an excitation wavelength of 369 nm ($\lambda_{emission}$ at 535 nm). This much shorter wavelength raises concern about UV-induced cell damage. This shortcoming of zinquin is shared by many other anthracene-, coumarin-, pyrene-, or dansyl-based sensors.[29] Longer wavelengths penetrate tissue better with less scattering, giving rise to higher resolution images, and do not require UV-grade optics in the fluorescence microscopes used to observe biological samples.

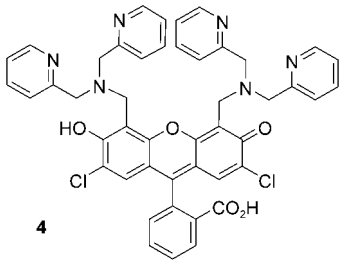

One other consideration in the design of chemosensors is matching of the $\lambda_{excitation}$ and $\lambda_{emission}$ with the laser and filter sets of the fluorescence microscopes to be used in the biological studies. Likewise, if co-staining experiments are to be performed, the optical properties of the sensor and the co-stains need to be distinctly different from each other to allow their independent probing. Chemosensors may be compared by using a sensitivity index based on the product of the quantum yield ϕ, that is, the ratio of emitted photons per photons used to excite a fluor, and the extinction coefficient ε of the sensor.[27] The higher the sensitivity index, the lower the sensor concentration required to obtain a signal.

Selectivity for zinc: In chemosensors for metal ions, the selectivity of the fluorescence response is achieved by a judicious choice of the metal binding site. Zinc is a borderline hard/soft metal with a variety of known coordination numbers, geometries, and donor atom sets.[2] This makes the design of zinc-selective chelates somewhat difficult, but the number and concentration of competing metal ions in biological systems is limited, simplifying the task in practice. Figure 3 shows the fluorescence response of the "zinc-selective" cyclen-appended coumarin-based sensor **5** upon addition of a range of metal ions.[30] In addition to zinc, the other divalent ions of Group 12 elicit a fluorescence response. Also, the soft-ion Pb^{2+} is found to bind. These results are typical for cyclen-, DPA-, or aminocarboxylate-based sensors, though exceptions are also known.[22] In the

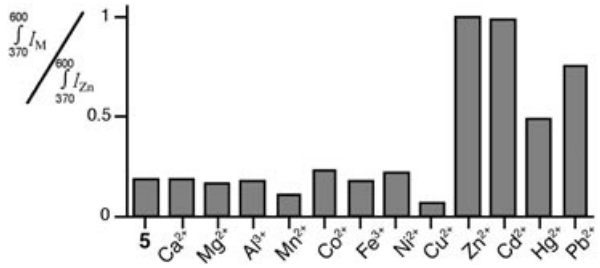

Figure 3. Metal-dependent relative integrated emission intensity increase after addition of a tenfold excess of metal to **5**. $\lambda_{excitation}$ at 345 nm, fluorescence measured after 30 h. For further experimental details, see Lim et al.[30] (figure used with permission).

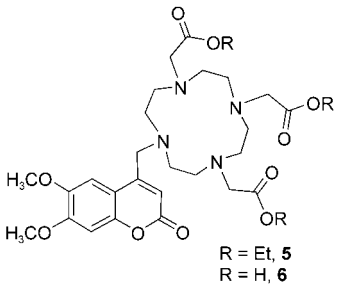

R = Et, **5**
R = H, **6**

biological setting, however, none of these toxic ions are expected to be present in any significant amount, excluding a false positive signal for zinc. On the other hand, the ions occurring in relatively large concentrations, such as Ca^{2+}, Mg^{2+} (and Na^{+}, K^{+}, not shown) do not bind to cyclen, and therefore do not induce any fluorescence, even when present in a large molar excess. Transition metals such as Mn^{2+}, $Fe^{2/3+}$, and Cu^{2+} bind to many cyclen, and DPA- or aminocarboxylate-based sensors.[31] However, they do not give a false positive fluorescence response as these paramagnetic ions quench the induced CHEF-type fluorescence. In a refined and more relevant experiment, it is necessary to investigate how Zn^{2+} ions directly compete with varying concentrations of other transition-metal ions for the sensor binding site.

Other zinc-specific sensors show different selectivity profiles, particularly the quinoline-based sensors which are much less susceptible to interference with metals such as Hg^{2+} or Cd^{2+}. The selectivity of the binding sites can, in principle, be improved by ligand designs that support or enforce square-pyramidal or trigonal-bipyramidal coordination modes, which are more readily accessible to Zn^{2+} than to most other transition metals.

Affinity for zinc: A fluorescence titration of a given sensor with Zn^{2+} identifies the zinc concentration range in which the sensor can be used to measure relative concentrations of zinc. If the zinc concentration is too low, no enhanced fluorescence is measured because no significant binding takes place. In the upper limit range, the sensor is saturated and cannot give any information about relative concentration changes of zinc (for other limitations in determining zinc concentrations using chemosensors, see below). Thus, every sensor is characterized by a useful working range of zinc concentrations. The ideal dissociation constant K_d of the sensor for the analyte should be a value close enough to the projected concentration of the analyte to allow monitoring of changes in its concentration.

Binding kinetics: If the temporal resolution of changing zinc concentrations is desired, it is obligatory that the reversible metal binding event to the sensor is adequately fast. For instance, the binding of Zn^{2+} to the cyclen-based sensor **5** is very slow ($t_{1/2} = 60$ min).[30] This is presumably due to the reorganization required to accommodate the metal in its convoluted binding site. Most sensors utilize non-macrocyclic polydentate chelates with fast binding kinetics. Rapidly binding sensors have been successfully used in time-resolved studies, as will be shown below.

pH-Dependence of the sensors: Protons potentially compete with zinc for the lone pair(s) of the Lewis basic metal binding site. If the lone pair responsible for the PET process gets protonated, it becomes also less available for the quenching process, and fluorescence is switched on even in the absence of the metal ion. Hence the working pH range for any chemosensor needs to be determined to allow a judgment whether the sensor can operate within the pH range expected in the biological system studied.[32]

Biodistribution properties: Ideally, the chemosensor is taken up by the cell or tissue, thus avoiding micro-injection techniques. An indication whether endocytotic mechanisms or passive diffusion through the cell membrane is responsible for the uptake of the sensor can be derived by observing the temperature-dependence of its uptake. If incubation of the cells with the sensor at 4 °C results in cell uptake, it provides a strong indication for a passive diffusion mechanism, since endocytosis at this temperature is greatly inhibited.[20] Once in the cell, the sensor may be excreted or metabolized, leading to gradually diminishing fluorescence.

The nature of pendant arms of the sensors can alter their uptake properties. For instance, it was proposed that the ester functionality on the more lipophilic zinquin ester **2** allows passive diffusion into the cell. It may also improve the retention of the probe inside cells, since the ester may be hydrolyzed by cytoplasmic esterases, with the resulting charged and more hydrophilic acid species unable to diffuse out.[33] Likewise, the sensor triacid **6** does not stain cells, whereas the triester **5** is taken up readily.[30] On the other hand, other zinquin derivatives that lack the ester functionality also get taken up,[20] indicating that while esterase-activated "prodrug" designs are an elegant way of manipulating the biodistribution properties of a sensor,[31] they are not a mandatory requirement for the making of successful intracellular zinc-specific stains.

Cell-permeable zinc chemosensors: A range of cultured mammalian cell types (e.g., mouse fibroblasts, rat pituitary tumor cells, COS, HeLa, Chinese hamster ovary cells) as well as yeast cells, exhibit punctuate staining patterns upon incubation with a number of structurally different, cell-permeable chemosensors (e.g., 2-Me-TSQ, **7**), as exemplified in Figure 4, recorded by O'Halloran and co-workers.[20] The nature of these discrete, intracellular, vesicular zinc pools remains unclear, but they appear to be an ubiquitous aspect of eukaryotic cell biology.[20]

A standard set of experiments is required to link the staining to intracellular zinc pools, and to minimize the potential for observing artifacts:[20]

1) The cells should show little or no fluorescence in the absence of the sensor.

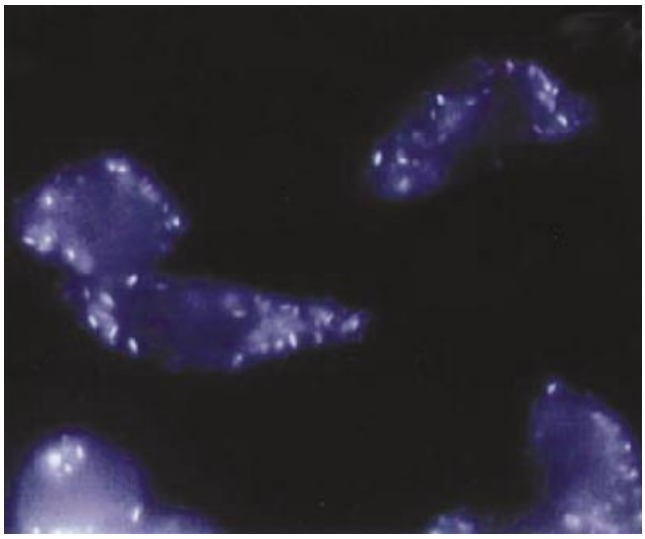

Figure 4. Microscopy images of mouse fibroblast cells by fluorescence in the presence of 10 μM sensor **7**. For further experimental details, see Nasir et al.[20] (figure used with permission).

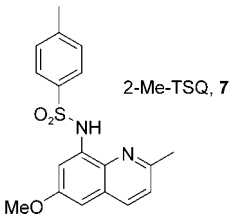

2) The observed stains should be sensitive to an exogenously altered zinc status of the cell. Addition of the ionophore pyrithione (2-mercaptopyridine *N*-oxide) in conjunction with exogenously added zinc is known to load the cells with zinc. Correspondingly, the observed fluorescence intensity of the stains should increase. Conversely, the addition of the membrane-permeable zinc scavenger TPEN (*N*,*N*,*N*′,*N*′-tetra(2-picolyl)ethylenediamine) to the cell culture reduces the intracellular "free" zinc concentration and, correspondingly, the observed fluorescence should diminish or vanish all together (see, for example, Figure 10 and Figure 13 later).
3) The staining should also be shown not to be due to sensor–zinc complexes preformed outside of the cell. Thus, the cell medium should be very zinc-poor or it should be shown that incubation of cells with the sensor–zinc complex does not result in any uptake or staining.[30]

Double-labeling experiments have identified some cell organelles in which select sensors preferentially accumulate. For instance, the sensor RhodZin-3 (**8**) has been shown to be selective for mitochondria in neurons (Figure 5).[34] On the other hand, the bright perinuclear staining pattern in COS cells using Zinpyr-1 (**4**) was found to be associated with acidic cell compartments identified as Golgi or Golgi-associated vesicles.[23,24]

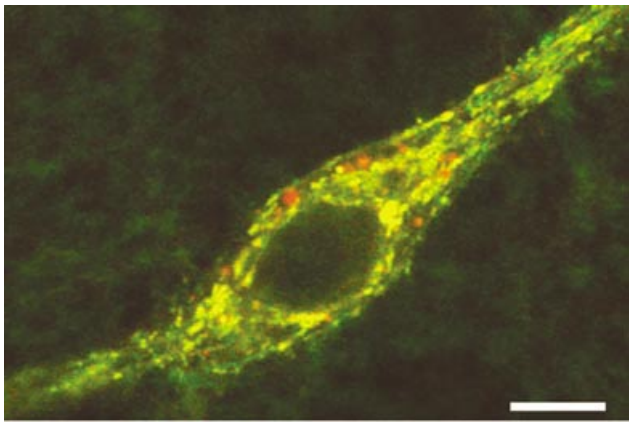

Figure 5. Co-localization of RhodZin-3 (**8**, red fluorescence) and the mitochondrial selective probe MitoTracker Green (green fluorescence) in cultured murine forebrain cells. Co-localization is indicated by the yellow color of the combined emission of the probes. For further experimental details, see Sensi et al.[34] (figure courtesy of K. R. Gee, used with permission).

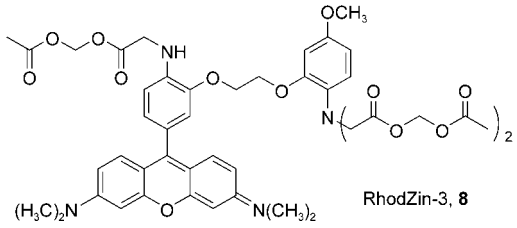

The ability to obtain images of zinc pools in cells, especially when using chemosensors of relatively low affinity for zinc, is surprising in light of the demonstrated absence of cytosolic "free" zinc pools in, for instance, *E. coli*.[11] However, since the nature of the observed zinc pools are not clear, it is too early to offer an explanation for this apparent discrepancy.

One caveat needs to be considered when using chemosensors to image zinc in cells or tissues. Each sensor can measure zinc only in the compartment(s) in which it accumulates. A lack of fluorescence enhancement in any given cell compartment does not necessarily imply that no zinc is present; it may merely mean that no sensor is present. Each sensor possesses unique biodistribution properties. This underlines the need for a range of sensors of varying biodistribution properties, in order to gain a comprehensive understanding of the distribution of zinc in cells.

Cell-impermeable zinc chemosensors: The utility of cell-permeable sensors for the imaging of cytosolic zinc is self-evident (for an example of the NO-triggered release of intracellular zinc, see Figure 10 below). However, non-cell-permeable dyes can also provide valuable biological information. For instance, it is known that insulin and Zn^{2+} are co-stored in pancreatic β-cells in secretory vesicles and are co-released by exocytosis. This process can be visualized by using the non-cell-permeable chemosensor FluoZin-3 (**9**).[35–37] Figure 6A shows the bursts of fluorescence ob-

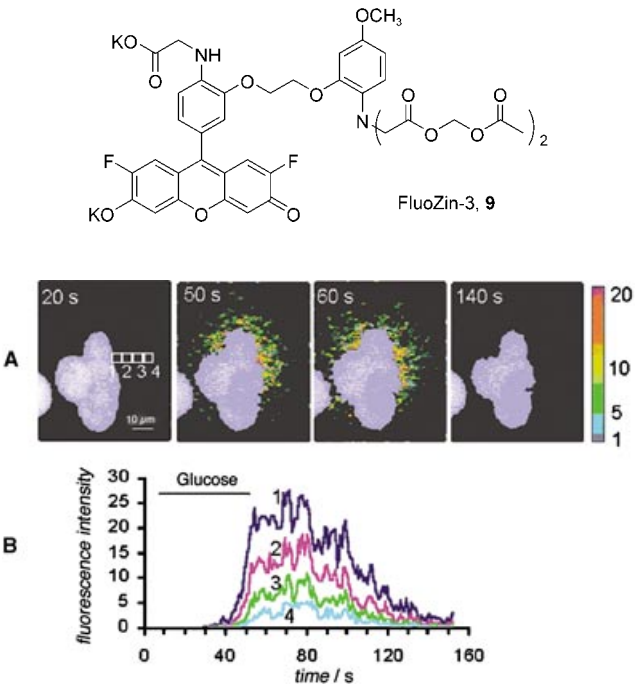

Figure 6. Imaging of Zn^{2+} secretion from pancreatic β-cells. Cells were incubated in buffer containing 2 μM FluoZin-3 (**9**) and stimulated to secrete by the application of 20 mM glucose (at 50 s). A: Colors indicate ratios of fluorescence intensities. B: The temporal responses of Zn^{2+} secretion were analyzed using the four regions of interest indicated as 1, 2, 3, 4 in A. For further experimental details, see Gee et al.[35] (figure used with permission).

served by Kennedy and co-workers following the addition of glucose to pancreatic β-cells.[35] The time-lapse images following the burst show the fluorescence decrease due to diffusional dilution of the zinc concentration.

Non-cell-permeable sensors have also been used to differentiate damaged from undamaged brain cells. Figure 7A shows a fluorescence microscopic image of a specific section

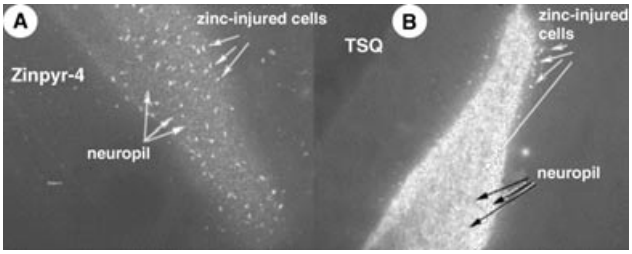

Figure 7. Hilus of dentate gyrus stained with Zinpyr-4, **10** (A) and TSQ, **1** (B). The brain tissue is taken from a rat following seizure activity. For further experimental details, see Burdette et al.[26a] (figure used with permission).

of brain tissue, stained with ZP4 (**10**), a non-cell-permeable, high-affinity zinc sensor from the Lippard laboratories.[26] The tissue was taken from rats after chemical-induced seizure. Distinctly visible are zinc-positive neurons, which are absent in tissue of animals which had not experienced a seizure. Figure 7B illustrates the advantage of using ZP4 (**10**) as compared to TSQ (**1**). This image is of much lesser diagnostic value. The identification of the damaged cells is made difficult because TSQ also stains Zn^{2+}-containing vesicles in the neuropil, the dense matrix interspersed among the nerve cells in the gray matter of the central nervous system.

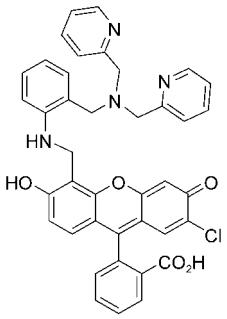

Single-wavelength excitation ratiometric zinc chemosensors: Currently, a most dynamic aspect in the development of zinc-specific chemosensors is the drive towards the realization of ratiometric sensors. The signal derived from a fluorescence microscopy image of a cell stained with a zinc-specific chemosensor allows the determination of the presence of zinc. Relative $\lambda_{emission}$ increases can reasonably be correlated with increases of $[Zn^{2+}]_{free}$, especially when the intensity has been shown to be modulated by externally induced changes of zinc availability (see above). However, the fluorescence quantum yield ϕ of the sensor is in most cases solvent-dependent. Since the solvent properties of the local environments in which the sensors accumulate are not known, the absolute $\lambda_{emission}$ measured cannot be correlated directly with a particular $[Zn^{2+}]_{free}$. However, the measurement of absolute $[Zn^{2+}]_{free}$ can be achieved by using a ratiometric sensor.

The principle of a ratiometric sensor is depicted in Figure 8. A ratiometric probe responds upon binding to an analyte with a shift in its $\lambda_{max\text{-}emission}$, which may or may not be concomitant with an increase in $\lambda_{emission}$. This $\lambda_{max\text{-}emission}$ shift should be enough to distinguish the $\lambda_{max\text{-}emission}$ of the co-existing Zn^{2+}-free and Zn^{2+}-bound species, allowing the determination of the ratio of $\lambda_{emission}$ of the Zn^{2+}-free to Zn^{2+}-bound species. Together with the known binding constant of the sensor, the unknown zinc concentration can be derived.[38] Assuming identical solvent influences on ϕ for the Zn^{2+}-free and Zn^{2+}-bound species, a ratiometric signal is internally calibrated. Further, neither light-source fluctuations nor photobleaching effects affect the signal ratio of bound to unbound sensor.

In principle, ratiometric-sensing behavior can be expected when the binding of the analyte changes the electronic properties of the chromophore. Ratiometric sensors for zinc are potentially very useful, but their realization is nontrivial. Consider, for instance, the rhodamine–fluoresceine hybrid dye **11**, introduced by Burdette and Lippard (shown in its

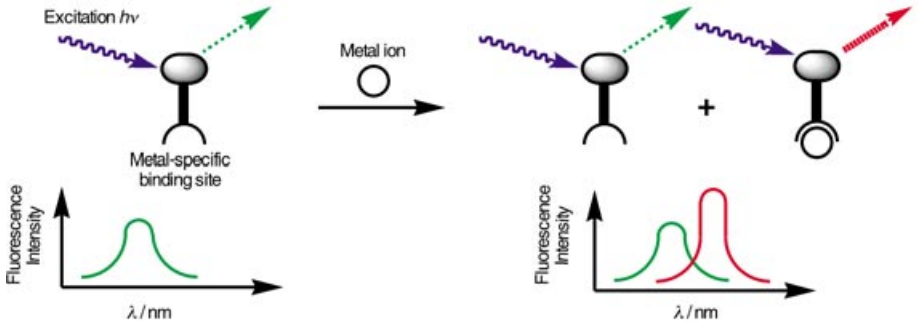

Figure 8. Schematic representation of the ratiometric measurement of metal concentration.

zinc-bound form **11-Zn**), in its two limiting resonance forms, aminoquinone **11-I** and iminophenoxide **11-II**.[25] Involvement of the amine functionality in the coordination to zinc

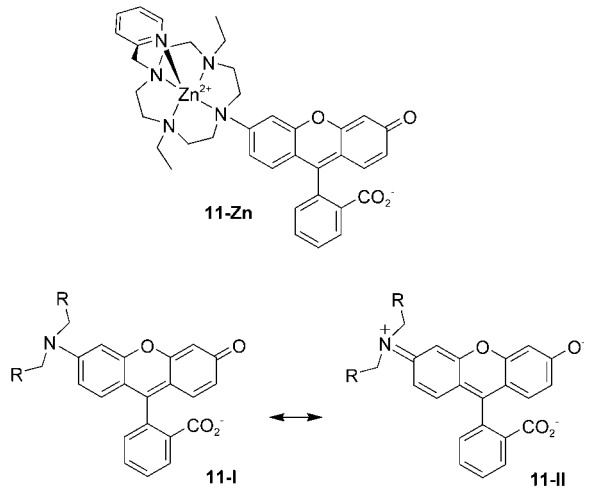

can reasonably be expected to shift the tautomeric equilibrium and, thus, the optical properties of the fluor. However, though **11** has been found to possess zinc chemosensory properties, it did not show any wavelength shift upon zinc binding. The explanation was found to lie in the high basicity of the chelate. Therefore, the sensor exists in a protonated state over a wide pH range, thus mimicking the presence of zinc and presumably also shifting the tautomeric equilibrium of the dye already to the aminoquinone form such that coordination to zinc causes no further shift.

The realization of a ratiometric sensor based on the zinc-induced shift of a tautomeric equilibrium was later accomplished by the group of Lippard using a less basic platform.[31] Phenoxynaphthoquinone **12-I** shares optical characteristics with naphthofluorescein, while its naphthoxyquinone tautomer **12-II** is fluorescein-like. Chemosensor **13** (ZNP1) was synthesized and its optical properties reveal two weak bands, footprints of both tautomeric forms (Figure 9). Coordination of **13** to zinc increases the overall fluorescence intensity of the sensor and, more significantly, it shifts the spectrum to one dominant broad peak, indicative of the phenoxynaphthoquinone tautomer **12-I**. This response provided the basis for the use of **13** in the single-excitation, dual-emission ratiometric sensing of zinc.

The biological value of this probe has been demonstrated. The diacetate derivative of **13** was found to be taken up by cells and, by using the standard tests described above, to be

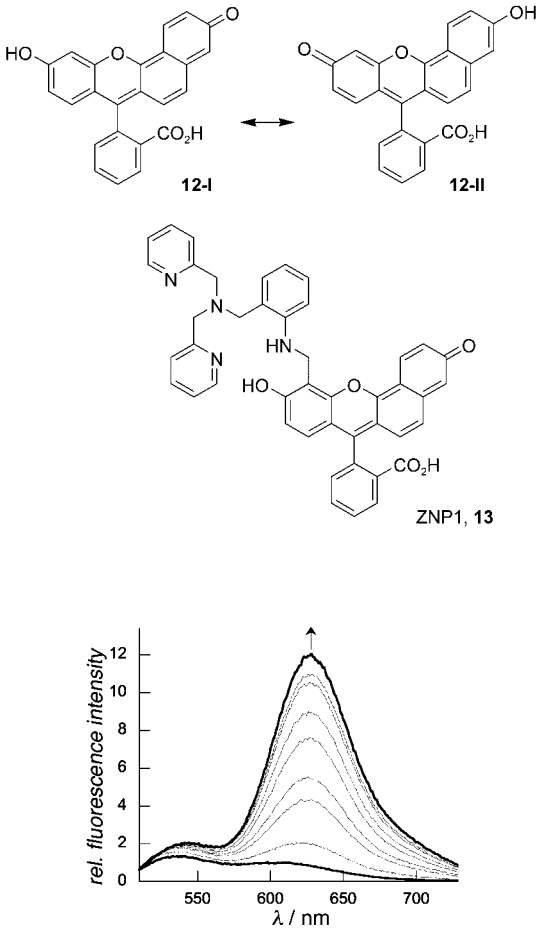

Figure 9. Ratiometric fluorescence spectroscopic response of ZNP1 to buffered Zn^{2+} solutions ($\lambda_{excitation}$ at 499 nm). For further experimental details, see Chang et al.[31] (figure used with permission).

suitable to measure changes in intracellular zinc concentrations in living mammalian cells. Figure 10 shows the images of live COS cells stained with ZNP1 acetate. The pseudocolors depict the ratio of the fluorescence intensities at the two emission wavelengths at 612 and 526 nm. The larger the ratio, the more zinc is present. In resting cells, little if any, "free", that is, imageable, endogenous zinc is present (Figure 10A). Figure 10B shows the result of the addition of *S*-

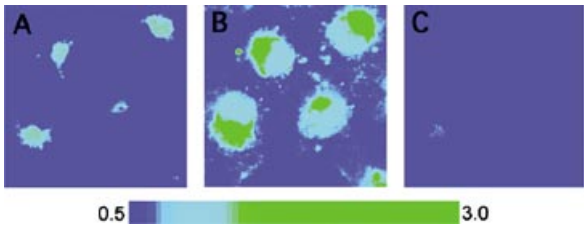

Figure 10. Ratio confocal fluorescence imaging of NO-triggered release of endogenous Zn^{2+} in live COS-7 cells. Fluorescence was collected in optical windows centered at 612 and 526 nm. Pseudocolor figures depict the ratio of fluorescence intensities at these two emission wavelengths. A: Incubation of cells with ZNP1-Ac. B: ZNP1-stained cells treated with *S*-nitrosocyctein. C: Reversal of the observed ratio increases with TPEN. For further experimental details, see Chang et al.[31] (figure used with permission).

nitrosocyctein, an NO-delivery agent. The ratio I_{612}/I_{526} increased, indicating the intracellular NO-triggered release of zinc. The cytosolic zinc was then chelated by TPEN, resulting in the complete loss of imageable zinc in the cells (Figure 11C). This experiment is a powerful demonstration of the ability of the signaling molecule NO to make Zn^{2+} available from tightly protein-bound, non-imageable zinc in the cytosol.

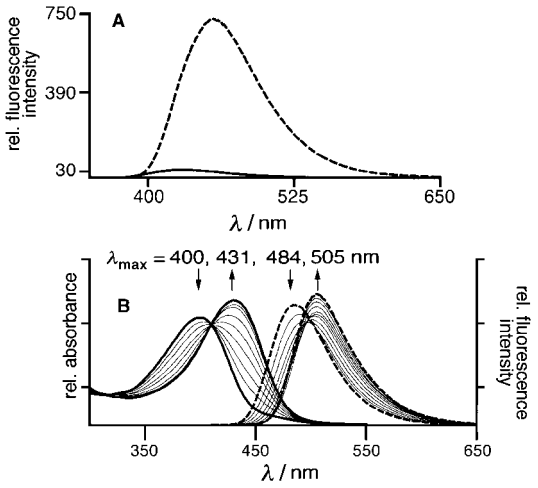

Figure 11. A: Solid trace: Emission spectrum of **14**; broken trace: **14** + 1 equiv Zn^{2+} (MeOH, $\lambda_{excitation}$ at 343 nm). B: Solid line, left spectra: UV-vis spectral titration of **15** with Zn^{2+} (0–1 equiv). Dashed line, right spectra: Fluorescence response upon titration of **15** with Zn^{2+} (0–1 equiv), $\lambda_{excitation}$ at 410 nm. For further experimental details, see Lim et al.[39] (figure used with permission).

The design of ratiometric sensors is fraught with many surprises, highlighting the fact that the design algorithm for sensors in general is not all understood. For instance, the DPA-derivatized (DPA = di(2-picolyl)amine) coumarin-based chemosensor **14** prepared by Lim and Brückner is structurally related to their sensor **5** discussed above, but utilizes an open-chain chelate.[39] This promised to alleviate the slow binding kinetics observed for the cyclen-based ana-

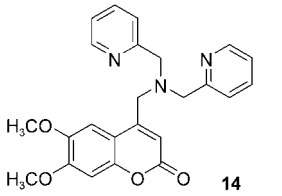

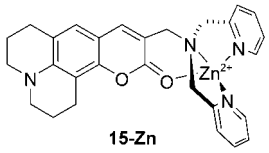

logue **5**. In fact, fast Zn^{2+}-binding characteristics were observed. Figure 11A shows the chemosensory response of sensor **14**. Addition of one equivalent of Zn^{2+} increases the integrated fluorescence intensity a surprising 23-fold as compared to the 4.4-fold increase observed for **5**. In a further development, the position of attachment of the DPA-ligand was moved from the 4-position in **14** to the 3-position of the coumarin framework, generating sensor **15**.[39] This shift is most important in the context of the design of a ratiometric sensor. The chelate attached directly adjacent to the lactone functionality of the coumarin framework allows the formation of the zinc complex **15-Zn** shown in which the three nitrogen atoms of the DPA and the lactone carbonyl oxygen atom coordinate to the Zn^{2+} ion (the coordination of one additional water molecule to complete a pseudo-trigonal-bipyramidal N_3O_2 coordination sphere around the metal ion in **15-Zn** cannot be excluded). This chelation mode may perturb the chromophore, giving rise to a ratiometric probe.

Figure 11B shows the results of spectrophotometric titrations of Zn^{2+} to a solution of **15**. Indeed, a ratiometric response was observed but the CHEF-type fluorescence increase was almost entirely lost. Further, the ratiometric response proved to be solvent dependent. The peak separation degrades presumably as the solvent competes with the carbonyl group for coordination to the metal center. Thus, the observed $\Delta\lambda_{max\text{-}emission}$ is only barely discernible in H_2O. This illustrates that the coordinating group on the fluor must not only be a crucial part of the chromophore, it must also be a competent ligand, withstanding the competition for the metal ion with the solvent and other potential donors present in biological media.

One intriguing approach toward the realization of a single-wavelength ratiometric sensor for Zn^{2+} relies on the cation-induced inhibition of excited state intramolecular proton transfer (ESIPT), most recently utilized by Fahrni and co-workers for the development of a ratiometric sensor for Zn^{2+}.[40,41] Certain chromophores, such as the 2-(2′-benzenesulfonamidophenyl)benzimidazole derivative **16-I**, undergo ESIPT to yield the emission of the proton-transfer tautomer **16-II**. This emission is generally highly Stokes' shifted. Removing the transferred proton by metal coordination (such as in **16-Zn**) makes ESIPT impossible. Since emission of the metal-coordinated species occurs with normal

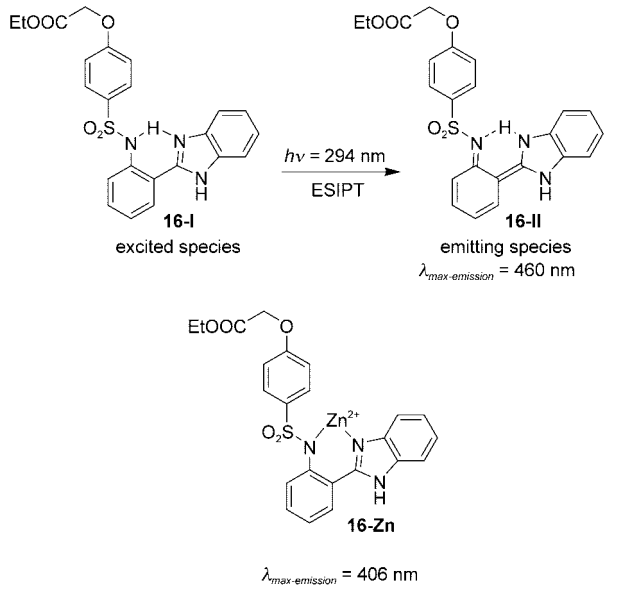

Stokes' shift, the wavelength separation of $\lambda_{max\text{-}emission}$ of the Zn^{2+}-bound and free base species can be expected to be large (here, 46 nm). Good separation of $\lambda_{max\text{-}emission}$ of the Zn-bound and unbound species allows for a simplified and potentially very sensitive ratiometric measurement. It is also important to note that using this concept, a modulation of $I_{emission}$ of the chromophores upon metal binding is not required, enabling the use of chromophores with a high ϕ and resulting in a bright sensor.

Dual-wavelength ratiometric zinc chemosensors: Woodroofe and Lippard have introduced an innovative approach to alleviate most of the problems associated with the design of a ratiometric probe operating by interference of the chromophore upon zinc binding.[42] The principle behind their two-fluorophore approach is illustrated in Figure 12. Two fluors

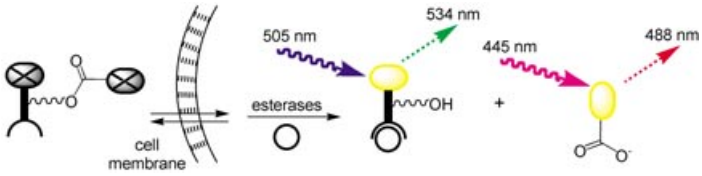

Figure 12. Schematic representation of the two-fluorophore approach to a ratiometric measurement of metal concentration.

are conjugated through an ester functionality. A conjugate is composed of a zinc-sensitive (the fluorescein-based sensor moiety, similar to Zinpyr-1, **4**) and a zinc-insensitive component (a coumarin moiety). The conjugate is essentially non-fluorescent and cell-membrane permeable. Once in the cell, esterases cleave the conjugate, separating the chemosensor and the coumarin, and rendering them both fluorescent in the process. Both fluors possess characteristic excitation and emission wavelengths. They can thus be probed independently of each other. Excitation of the coumarin (at 445 nm) and measurement of the emission intensity at 488 nm provides information on the concentration of cleaved sensor. Measurement of the emission intensity at 534 nm (excitation at 505 nm) affords information about the amount of zinc present. In the absence of zinc, the ratio of the emission intensity I_{534}/I_{488} is 0.5 and it increases to 4.0 upon saturation of the chemosensor with zinc.

Figure 13 shows the results of a dual filter microscopy experiment.[42] HeLa cells were incubated with conjugate **17**. Figure 13B shows the image resulting from the specific excitation of the coumarin and the measurement of its emission, while Figure 13C shows the image resulting from a chemosensor-specific excitation/emission. Increase of the intracellular zinc concentration increased the emission intensity at 543 nm, but not that recorded at 488 nm. While the intensity ratio was not correlated to an absolute zinc concentration, the result demonstrates the co-localization of the fluors. The esterase processing of the conjugate generates the two fluors in an exact 1:1 ratio. The presence of a defined ratio of co-localized sensors is an essential condition for ratiometric sensing.

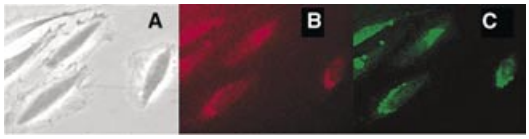

Figure 13. Phase contrast (A) and fluorescence (B, C) microscopy images of HeLa cells incubated with Coumazin-1 (**17**) with the addition of $ZnCl_2$ and sodium pyrithione. Fluorescence images were acquired with $\lambda_{excitation}$ at 400–440 nm, band-pass of 475 nm (B) or with $\lambda_{excitation}$ at 460–500 nm, band-pass of 510–560 nm (C). For further experimental details, see Woodroofe et al.[42] (figure used with permission).

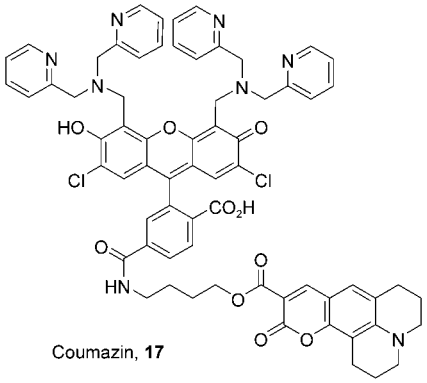

Two-photon (ratiometric) sensors: Instead of only being able to absorb one photon of a certain wavelength to reach an excited state, some chromophores possess the ability to absorb simultaneously two photons of double the wavelength (half the energy) to reach the same excited state.

Identical fluorescence is observed upon relaxation of the chromophore back to the ground state, irrespective of the means by which the excited state was reached. Two-photon absorption is a nonlinear optical property due to its quadratic dependence on the intensity of the incident light. This nonlinearity allows for high spatial resolution of the absorption (and, therefore, the fluorescence) event.[43] This recommends two-photon dyes for use in single-molecule detection devices and three-dimensional sub-micron resolution imaging techniques in fixed and living tissues.

The use of two-photon dyes absorbing especially in the range above 700 nm has a number of practical advantages:

1) Use of commercial near-IR femtosecond sources; the fs pulse also minimizes photo-damage to the tissue under investigation.
2) Good tissue penetration of the excitation and emission photons.
3) High spatial resolution allowing the excitation of femtoliter focal volumes.
4) Low background signal, as few materials would be expected to undergo multi-photon events at these wavelengths.

Thus, for the purpose of obtaining high-resolution images of zinc distribution in, for example, thick tissue sections, the development of fluorescent sensors for zinc with appreciable two-photon absorption cross sections is desirable.

O'Halloran and co-workers have introduced an example of a zinc-specific chemosensor suitable for two-photon microscopy.[44] Moreover, the sensor benzoxazole (Zinbo-5, **18**) proved to exhibit a ratiometric response (Figure 14A). This allows the construction of a plot of the zinc-concentration dependence of the intensity ratio of the λ_{max} of the zinc-free (407 nm) and zinc-bound species (443 nm), see Figure 14B (excitation was performed with one wavelength near the isosbestic point, thus exciting both species equally well). The ratiometric response of the sensor is also the basis for the recording of pseudocolor images such as those obtained of fibroblast cells stained with **18**, shown in Figure 14D–F. The varying ratios of $I_{emission}$ at 445 and 402 are color coded, showing clearly the effects of the externally induced variation of the zinc status of the cells.[44]

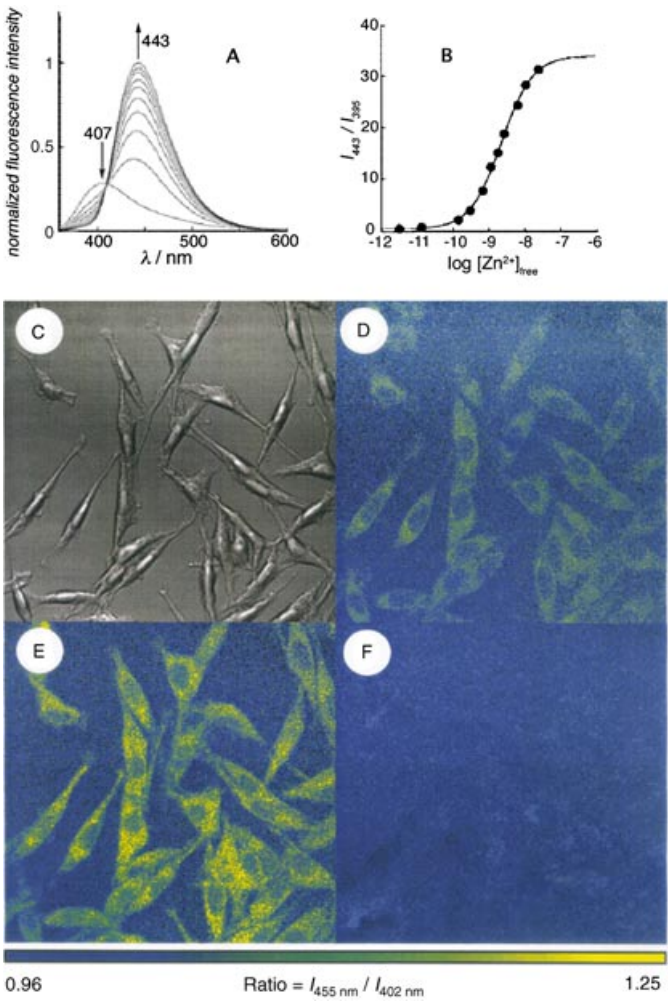

Figure 14. A: Emission spectra of Zinbo-5 (**18**), $\lambda_{excitation}$ at 356 nm in a Zn^{2+}-buffered system. B: Plot of the fluorescence intensity ratio I_{443}/I_{395}. C-F: Emission ratio images of fibroblast [L(TK)$^-$] cells in Zinbo-5 (**17**). C: Brightfield transmission image. D: Ratio of images collected at $\lambda_{emission}$ at 445 and 402 nm. E: Ratio image following treatment with Zn^{2+}/pyrithione, followed by wash with Zinbo-5 (**17**) stock. F: Ratio image of the same field after treatment with TPEN. For further experimental details, see Taki et al.[44] (figure used with permission).

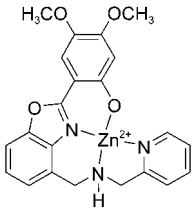

Zinbo-5, **18-Zn**

Conclusions

In summary, the quest to learn more about zinc biochemistry has spawned significant conceptual advances in the design of zinc-selective chemosensors, and their application to interrogate biological systems in a remarkably short time span. The emergence of the field of metalloneurochemistry is but one impressive example of how the contributions of bioinorganic chemist can advance the knowledge of biological systems.[45,46] The synthetic and mechanistic basis for the synthesis of sensors with varying photophysical, binding, and biodistribution properties continues to be developed. As known and novel sensors are utilized to interrogate biological systems, there is no doubt that chemosensors will continue to significantly further the knowledge of the biochemistry of zinc.

Acknowledgement

This work was supported by the UConn Research Foundation. We thank Professors Vijay Kumar, Bob Michel (both Department of Chemistry) and Steven Zinn (Department of Animal Sciences), the "Zinc Group" at the University of Connecticut, for useful discussions.

[1] a) B. L. Vallee, K. H. Falchuk, *Physiol. Rev.* **1993**, *73*, 79; b) H. Vahrenkamp, *Chem. Unserer Zeit*, **1988**, *22*, 73.
[2] D. S. Auld, *Biometals* **2001**, *14*, 271.
[3] J. H. Laity, B. M. Lee, P. E. Wright, *Curr. Opin. Struct. Biol.* **2001**, *11*, 39.
[4] A. S. Prasad, *Am. J. Clin. Nutr.* **1991**, *53*, 403.
[5] M. de Onis, E. A. Frongillo, M. Blossner, *Bull W. H. O.* **2000**, *78*, 1222.
[6] P. A. Walravens, N. F. Krebs, K. M. Hambidge, *Am J. Clin. Nutr.* **1983**, *38*, 195.
[7] M. E. Scott, K. G. Koski, *J. Nutr.* **2000**, *130*, 1412S.
[8] L. A. Gaither, D. J. Eide, *Biometals* **2001**, *14*, 251.
[9] W. Maret, *Biometals* **2001**, *14*, 187.
[10] L. A. Finney, T. V. O'Halloran, *Science* **2003**, *300*, 931.
[11] C. E. Outten, T. V. O'Halloran, *Science* **2001**, *292*, 2488.
[12] C. E. Outten, T. A. Tobin, J. E. Penner-Hahn, T. V. O'Halloran, *Biochemistry* **2001**, *40*, 10417.
[13] Y. Hitomi, C. E. Outten, T. V. O'Halloran, *J. Am. Chem. Soc.* **2001**, *123*, 8614.
[14] For recent reviews see: a) E. Kimura, T. Koike, *Chem. Soc. Rev.* **1998**, *27*, 179; b) E. Kimura, S. Aoki, *BioMetals* **2001**, *14*, 191; c) C. Frederickson, *Sci. STKE* **2003**, pe18 (DOI: 10.1126/stke.2003.182.pe18); d) P. Jiang, Z. Guo, *Coord. Chem. Rev.* **2004**, *248*, 205; e) K. Kikuchi, K. Komatsu, T. Nagano, *Curr. Opin. Chem. Biol.* **2004**, *8*, 182.
[15] H. C. Freake, M. Schaller, A. Trzcienski, S. A. Zinn, *Proc. Nutr. Soc.* **2002**, *61*, 47A.
[16] A. W. Czarnik, *Acc. Chem. Res.* **1994**, *27*, 302.
[17] A. P. de Silva, D. B. Fox, H. J. M. Huxley, T. S. Moody, *Coord. Chem. Rev.* **2000**, *205*, 41.
[18] R. P. Haugland, *Handbook of Fluorescent Probes and Research Chemicals*, Molecular Probes, Eugene, **2002**.
[19] R. Y. Tsien, in *Calcium As a Cellular Regulator* (Eds.: E Carafoli, C. B. Klee), Oxford University Press, New York, NY, **1999**, p. 28.
[20] a) M. S. Nasir, C. J. Fahrni, D. A. Suhy, K. J. Kolodsick, C. P. Singer, T. V. O'Halloran, *J. Biol. Inorg. Chem.* **1999**, *4*, 775; b) K. M. Hendrickson, J. P. Geue, O. Wyness, S. F. Lincoln, A. D. Ward, *J. Am. Chem. Soc.* **2003**, *125*, 3889.
[21] C. J. Fahrni, T. V. O'Halloran, *J. Am. Chem. Soc.* **1999**, *121*, 11448.
[22] a) T. Gunnlaugsson, T. C. Lee, R. Parkesh, *Org. Biomol. Chem.* **2003**, *1*, 3265; b) for an example of a conformationally regulated Zn^{2+} versus Cd^{2+} selectivity, see: A. M. Costero, S. Gil, J. Sanchis, S. Peransí, V. Sanz, J. A. G. Williams, *Tetrahedron*, **2004**, *60*, 6327.
[23] G. K. Walkup, S. C. Burdette, S. J. Lippard, R. Y. Tsien, *J. Am. Chem. Soc.* **2000**, *122*, 5644.
[24] S. C. Burdette, G. K. Walkup, B. Springler, R. Y. Tsien, S. J. Lippard, *J. Am. Chem. Soc.* **2001**, *123*, 7831.
[25] S. C. Burdette, S. J. Lippard, *Inorg. Chem.* **2002**, *41*, 6816.
[26] a) S. C. Burdette, C. J. Frederickson, W. Bu, S. J. Lippard, *J. Am. Chem. Soc.* **2003**, *125*, 1778; b) C. J. Frederickson, S. C. Burdette, C. J. Frederickson, S. L. Sensi, J. H. Weiss, H. Z. Yin, R. V. Balaji, A. Q. Truong-Tran, E. Bedell, D. S. Prough, S. J. Lippard, *J. Neurosci. Methods* **2004**, *139*, 79.
[27] D. A. Pearce, N. Jotterand, I. S. Carrico, B. Imperiali, *J. Am. Chem. Soc.* **2001**, *123*.
[28] N. Jotterand, D. A. Pearce, B. Imperiali, *J. Org. Chem.* **2001**, *66*, 3224.
[29] For the latest examples, see: a) G. Nishimura, Y. Shiraishi, T. Hirai, *Ind. Eng. Chem. Res.* **2004**, *43*, 6064; b) Y. Chen, D. X. Zeng, *ChemPhysChem*, **2004**, *5*, 564; c) Z. Wu, Q. Chen, G. Yang, C. Xiao, J. Liu, S. Yang, J. S. Ma, *Sens. Actuators B*, **2004**, *99*, 511; d) The sensors reviewed in reference [14].
[30] N. C. Lim, L. Yao, H. C. Freake, C. Brückner, *Bioorg. Med. Chem. Lett.* **2003**, *13*, 2251.
[31] C. J. Chang, J. Jaworski, E. M. Nolan, M. Sheng, S. J. Lippard, *Proc. Natl. Acad. Sci. USA* **2004**, *101*, 1129.
[32] S. Aoki, S. Kaido, H. Fujioka, E. Kimura, *Inorg. Chem.* **2003**, *42*, 1023.
[33] I. B. Mahadevan, M. C. Kimber, S. F. Lincoln, E. R. T. Tiekink, A. D. Ward, W. H. Betts, I. J. Forber, P. D. Zalewski, *Aust. J. Chem.* **1996**, *49*, 561.
[34] S. L. Sensi, D. Ton-That, J. H. Weiss, A. Rothe, K. R. Gee, *Cell Calcium* **2003**, *34*, 281.
[35] K. R. Gee, Z.-L. Zhou, W.-J. Qian, R. Kennedy, *J. Am. Chem. Soc.* **2002**, *124*, 776.
[36] W.-J. Qian, R. T. Kennedy, *Biochem. Biophys. Res. Commun.* **2001**, *286*, 315.
[37] W.-J. Qian, C. A. Aspinwall, M. A. Battiste, R. T. Kennedy, *Anal. Chem.* **2000**, *72*, 711.
[38] J. R. Lakowicz, *Principles of Fluorescence Spectroscopy*, 2nd ed., Kluwer Academic/Plenum, New York, **1999**.
[39] N. C. Lim, C. Brückner, *Chem. Commun.* **2004**, 1094.
[40] C. J. Fahrni, M. M. Henary, D. G. VanDerveer, *J. Phys. Chem. A* **2002**, *106*, 7655.
[41] M. M. Henary, Y. Wu, C. J. Fahrni, *Chem. Eur. J.* **2004**, *10*, 3015.
[42] C. C. Woodroofe, S. J. Lippard, *J. Am. Chem. Soc.* **2003**, *125*, 11458.
[43] K. Belfield, D. , K. J. Schafer, Y. Liu, X. Ren, E. W. Van Stryland, *J. Phys. Org. Chem.* **2000**, *13*, 837.
[44] M. Taki, J. L. Wolford, T. V. O'Halloran, *J. Am. Chem. Soc.* **2004**, *126*, 712.
[45] S. C. Burdette, S. J. Lippard, *Proc. Natl. Acad. Sci. USA* **2003**, *100*, 3605.
[46] H. H. Sandstead, C. J. Frederickson, J. G. Penland, *J. Nutr.* **2000**, *130*, 496S.

Published online: October 14, 2004

